

# Positioning Controller for Mechanical Systems with a Mini Harmonic Drive Servo Actuator

Tegoeh Tjahjowidodo, Farid Al-Bender, Hendrik Van Brussel, and Wim Symens

**Abstract**— Harmonic drives (HD) are high-ratio, compact torque transmission systems. However, due to frictional effects and internal flexibility, a HD shows unique (torsional) stiffness behavior characterized by a stiffening spring in parallel with a hysteresis element, which is modeled using the Maxwell-slip model. As a result of this complex nonlinear behavior, a classical linear control strategy obviously does not perform very well, in a system with HD component, for achieving accurate positioning. This paper aims to characterize the dynamic behavior in mechanical system with HD and, more specifically, to use this knowledge to design effective control schemes. Modeling of the system is achieved via the Describing Function approach, applied to the hysteresis element, to yield the stiffness and damping in function of the amplitude of motion. Afterwards, a nonlinear feedback control strategy, utilizing a gain scheduling obtained from the aforementioned model-based identification, is implemented for compensating the error. The results show high performance in regard to rise time, positioning error and robustness as compared to a conventional cascade controller.

## I. INTRODUCTION

INVENTED by Walton Musser in 1955, primarily for aerospace applications, harmonic drives are high-ratio, compact torque transmission systems. As shown schematically in Fig. 1, this nascent mechanical transmission, occasionally labeled ‘strain-wave gearing’, employs a continuous deflection wave along a non-rigid gear, the so-called ‘flexspline’, to allow gradual engagement of gear teeth. Besides a thin-walled flexible cap with small external gear of the flexspline, a harmonic drive (HD) also contains two other important components, namely a wave-generator, which is a ball-bearing assembly with a rigid elliptical inner-race, and a circular-spline (sometimes it is split into two circular-splines), a rigid ring with internal teeth machined along a slightly larger pitch diameter than that of the flexspline.

Manuscript received January 15, 2007.

T. Tjahjowidodo was with PMA/Katholieke Universiteit Leuven, Belgium. He is now with the Flanders’ MECHATRONIC Technology Centre, Celestijnenlaan 300D, 3001 Leuven, BELGIUM (phone: +32-16-328041; fax: +32-16-328064; e-mail: tegoeh.tjahjowidodo@fmct.be).

F. Al-Bender is with the Department of Mechanical, Division PMA, Katholieke Universiteit Leuven, Celestijnenlaan 300B, 3001 Leuven, BELGIUM (e-mail: farid.al-bender@mech.kuleuven.be).

H. Van Brussel is with the Department of Mechanical, Division PMA, Katholieke Universiteit Leuven, Celestijnenlaan 300B, 3001 Leuven, BELGIUM (e-mail: hendrik.vanbrussel@mech.kuleuven.be).

W. Symens is with the Flanders’ MECHATRONIC Technology Centre, Celestijnenlaan 300D, 3001 Leuven, BELGIUM (e-mail: wim.symens@fmct.be).

When properly assembled, the wave-generator is nested inside the flexspline, causing the flexible gear-tooth circumference on the flexspline to adopt the elliptical profile of the wave-generator. While the wave-generator is rotated, the engagement of the external teeth of the flexspline to the internal teeth of the circular spline will cause highly reduced rotation of the circular spline. Through this unconventional mechanism, gear ratios up to 500:1 can be achieved in a single transmission step.

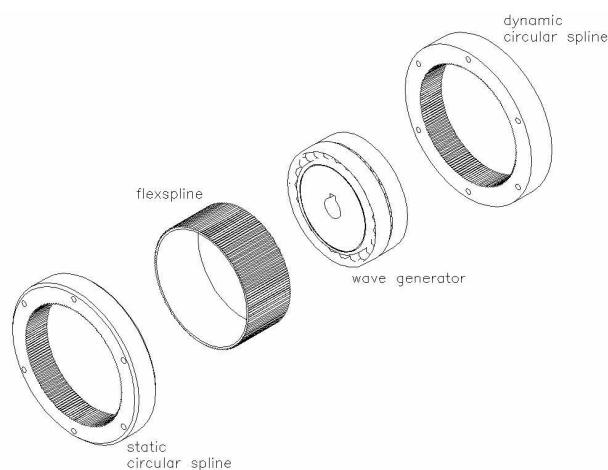


Fig. 1. Schematic drawing of harmonic drive components.

Ideally a HD transmission can be treated as a rigid gear reduction system. However, due to the relatively high flexibility of the flexspline, a HD shows unique (torsional) stiffness behavior [1,2]. A typical shape of the torsional stiffness consists of two characteristic properties: an increasing stiffness with displacement and a hysteresis loss as seen in Fig. 2 [3].

In order to capture this nonlinear stiffness behavior, the manufacturers suggest using piecewise linear approximations whereas several independent researchers [4,5] prefer a cubic polynomial approximation. The hysteresis loss in a HD is a phenomenon more difficult to model than the stiffness, yet sometimes it is ignored. Taghirad [6] proposed an advanced hysteresis model of torsional stiffness in the flexspline. He assumed that the hysteresis mainly came from the structural damping of the flexspline. Seyfferth *et al.*[7] offered to model the hysteresis as a combination of Coulomb friction and a weighted friction function, represented by a hyperbolic

function to capture the pre-sliding friction behavior, while Tjahjowidodo *et al.* [3] proposed to make use of the pre-sliding friction model to capture the hysteresis losses in the torsional stiffness of harmonic drive.

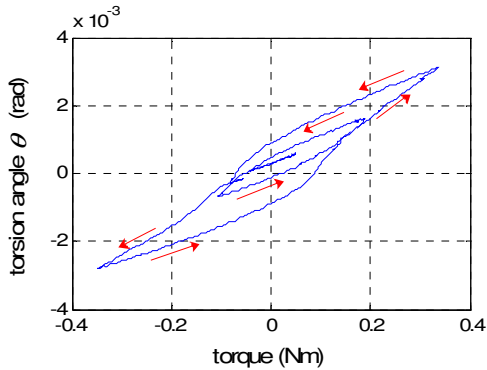


Fig. 2. Typical torsional stiffness profile.

As a result of the complex behavior, a classical linear control strategy obviously does not perform very well in a system with HD component for achieving accurate positioning. In several robotic control techniques such as feedback linearization, computed torque method, and some adaptive control schemes, the actuator torque is taken to be the control input. Consequently, torque measurement is obligatory in this system, since the compensation is accomplished through the feedback of the torque. Taghirad [8,9] measured the transmitted torque through the HD for the purpose of feedback compensation and utilized a Kalman filter to observe the torque. Similarly to that, Dhaouadi [10] proposed a nonlinear observer for forecasting the non-measurable friction to provide asymptotic stability and position tracking of the system.

Another approach to compensate the tracking error in HD systems is proposed by Hauschild *et al.* [11]. They assumed the absence of backlash-like torsional stiffness and used a model based on classical friction to compensate the error in HD systems in feedforward compensation.

This paper aims to characterize the dynamic behavior in mechanical system with HD and, more specifically, to use this knowledge to design effective control schemes. Modeling of the system is first outlined. Afterwards, a nonlinear feedback control strategy, utilizing a gain scheduling controller based on the knowledge obtained from identification is implemented for compensating the error.

In the following, section 2 describes the experimental setup and outlines the scope of this work. Section 3 and 4 discusses the system modeling and the control strategies that are used for positioning controller purpose. These sections also present and discuss the obtained results. Finally, appropriate conclusions are drawn in section 5.

## II. EXPERIMENTAL SETUP

The most recent design of harmonic drive, namely FHA-C mini servo actuator, combines the gear set with an AC servo motor in one compact package. The AC servo motor with permanent magnets and 5 pairs of poles provides torque without the often annoying brush wear and friction. This component is also equipped with an encoder mounted to the output of the motor (before the gear transmission) with a resolution of 8000 pulses per revolution to provide position feedback to the servo controller.

For measuring the displacement output from the gear transmission, a K-1 laser rotary encoder from Canon™ is connected to the system through a flexible coupling. This high-accuracy encoder gives 81000 pulses per revolution, each pulse having 16 interpolated positions, resulting in an incremental angular displacement encoder with 1.296.000 pulses per revolution. Fig. 3 shows the test setup.

As the FHA-C mini servo actuator is presented in a compact, small package, with an integrated AC servo motor and high-resolution encoder, it makes the assembling of the component in a mechanical system relatively easy to accomplish. However, its compactness introduces difficulties in identifying the dynamic behavior of the system. For instance, the friction in the motor cannot be identified separately from the torsional stiffness of the gearing system. Separate models of the torsional stiffness and friction can only be provided by the manufacturer.

Schematically, the dynamic behavior of the system can be represented as in Fig. 4, where the system is driven by an applied torque from the motor,  $T$ , and the servo motor itself is subjected to a frictional torque,  $T_F$ . The output of the motor is connected to the input side of the gearing system, namely the wave generator, through a shaft which has certain linear stiffness ( $k_S$ ) exerting torsional torque,  $T_S$ . The gear system transmits the (hysteresis) torsional torque through the gear meshing in the flexspline and the circular-spline,  $T_H$ , through a hysteretic spring,  $k_H$ .

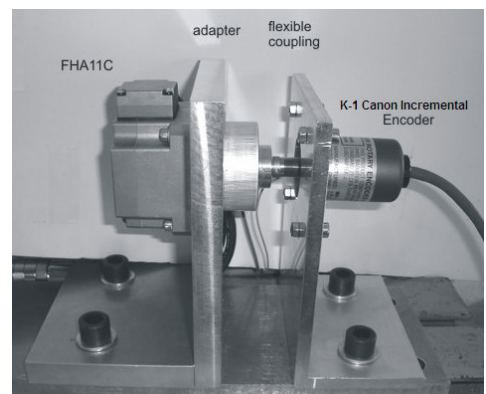


Fig. 3. Experimental apparatus of FHA-C mini servo actuator.

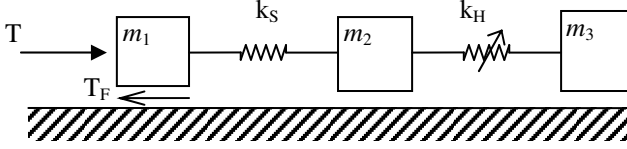


Fig. 4. Schematic drawing of the FHA-C mini servo actuator.

Due to the difficulty in the modeling of the dynamic parameters of each component in the system apparatus separately, including the friction in the motor armature, the shaft stiffness and the torsional stiffness of the gear transmission, the system will be modeled using two semi grey box model approaches. The first approach considers the system as a single lumped mass subjected to a frictional surface. The second approach takes into account the torsional stiffness with hysteresis, which is apparent in harmonic drive systems. Afterwards, these two different models will be used as the basis for designing the control strategies.

The setup will be considered as for a point-to-point application system, while the controllers are designed based on the following performances: short settling time and minimal overshoot.

### III. FIRST APPROACH CONTROLLER

This approach neglects the complexity in the internal system under investigation. The system will be considered as an actuated inertia system resting on a (hysteresis) frictional surface as shown in Fig. 5.

The first step of modeling this system is to obtain the hysteresis characteristics of the pre-sliding friction. The simplest way to perform this task is by exciting the system with periodic signals at certain amplitude and low frequency in order to minimize the effect of the inertia force. Fig. 6 depicts the hysteresis of the pre-sliding friction torque, when the system is excited by sinusoidal velocity input at 0.003 rad/s and 0.2 Hz. The horizontal axis represents the displacement measured by the output encoder, while the vertical one denotes the friction torque. The dashed-line represents the hysteresis of the actual friction torque, while the solid-line is the fitted friction torque utilizing an exponential continuous function of displacement (so-called a virgin curve),  $T_f = h_0(1 - \exp(-a\theta^d))$ . By using a least square fit, the obtained parameters are  $h_0 = 0.15$  Nm,  $a = 636$  and  $d \approx 1$ .

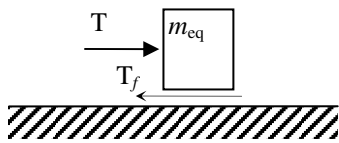


Fig. 5. First approach model of the setup.

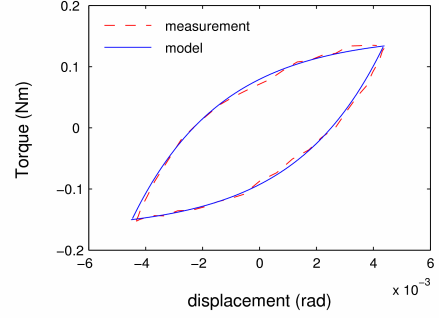


Fig. 6. The hysteresis loop of the pre-sliding friction force.

For the purpose of designing position control, we implement a gain scheduling technique as presented in [12,13]. The general idea of the gain scheduling controller is to adjust the controller gains based on the varying dynamic parameter of the system. Al-Bender *et al.* [14] formulated the equivalent dynamic parameters of the system subjected to the considered “hysteretic springs”, which can be modeled by the original Maxwell-slip [15]. They use the classical approach of the describing function [16] to obtain equivalent stiffness and damping of the system with hysteretic springs analytically. The equivalent dynamic parameters are then formulated as follows:

$$k_e = -\frac{4}{A\pi} \int_0^{\pi} y\left(\frac{A}{2}(1 - \cos(\theta))\right) \cdot \cos(\theta) \cdot d\theta \quad (1)$$

$$c_e \omega = -\frac{8}{\pi A^2} \int_0^{\pi} \left( y(\theta) - \frac{y(A)}{2} \right) \cdot d\theta \quad (2)$$

where  $A$  is the amplitude of the motion and  $y(\theta)$  is the virgin curve of the hysteresis, which characterizes the behavior of pre-sliding friction as function of displacement,  $\theta$ , when relative motion takes place for the first time. Based on the identified parameters from the previous section, the model of the virgin curve can be obtained. Utilizing (1) and (2), the equivalent dynamic parameters as functions of amplitude of motion as described previously can then be calculated.

The gain scheduling (GS) controller consists of two different modes and it switches between those modes corresponding to the pre-sliding and the gross sliding regimes, respectively, the gain needs to be scheduled only in the first mode, i.e. within a certain stroke after every motion reversal, discretely.

Utilizing the obtained equivalent dynamic parameters as shown in Fig. 7, we optimize the PD gains at different selected parameters (amplitudes of motions) considering the designated performance criteria. Subsequently, the optimal gains are interpolated, resulting in the gain scheduling shown in Fig. 8.

As a result, Fig. 9 shows the step response to a 0.4 rotation step input ( $0.4 \times 2\pi$  rad  $\approx 2.513$  rad) of the system, without load, utilizing the gain scheduling controllers. As a

comparison we also implemented a cascade (position and speed loop) controller, which is very popular for eliminating frictional effects in practical applications. Both controllers give low steady-state errors, approximately  $8.8 \times 10^{-4}$  rad. Observing the step responses in Fig. 9, we can see that the gain scheduling controller offers a faster response compared to the cascade controller.

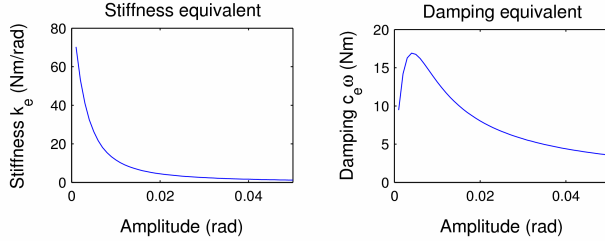


Fig. 7. The dynamic equivalent parameters of the friction.

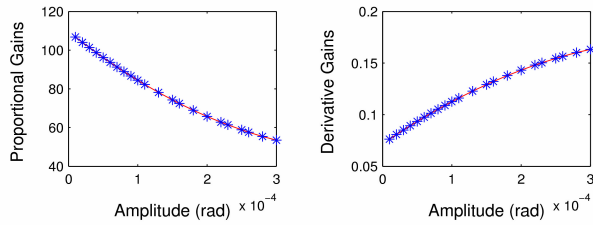


Fig. 8. Scheduled PD gains developed based on the equivalent dynamic parameters according to the first model.

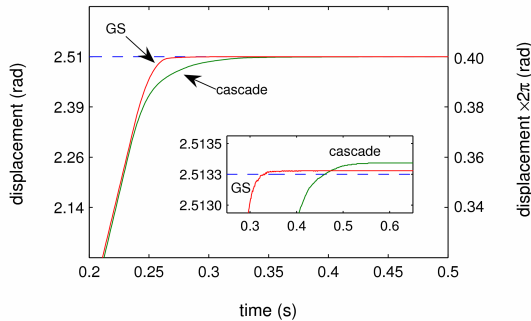


Fig. 9. Step response to a 2.513 rad step input of the system with the gain scheduling (GS) and the cascade controllers.

In order to evaluate the effectiveness of the controller and robustness against inertia and friction variations, the same controllers are also applied to load inertia. An aluminium disc with diameter of 120 mm and thickness of 10 mm, yielding a moment of inertia of approximately  $5.3 \times 10^{-4}$   $\text{kgm}^2$ , is mounted on the output shaft. Fig. 10 shows the step response to a 2.513 rad step input. The proposed gain scheduling controller results in the shortest rise time and provides a better accuracy compared to the cascade controller. The performances for each controller under different conditions are tabulated in Table I.

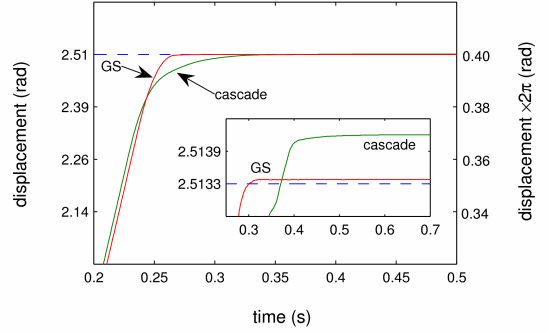


Fig. 10. Step response to a 2.513 rad step input of the loaded system with the gain scheduling (GS) and the cascade controllers.

TABLE I.  
PERFORMANCE COMPARISON OF THE CONTROLLERS.

Object	Step input (rad)	Controller	Rise time <sup>1</sup> (s)	Error (rad)
No Load	2.513	GS	0.24	$0.388 \times 10^{-4}$
		Cascade	0.28	$1.131 \times 10^{-4}$
Loaded	2.513	GS	0.25	$0.969 \times 10^{-4}$
		Cascade	0.29	$8.870 \times 10^{-4}$

<sup>1</sup> The time to take the system to within 1% of the set point.

#### IV. SECOND APPROACH CONTROLLER

The second approach of modeling considers the FHA-C mini actuator system as a semi grey box model, where the applied torque,  $T$ , drives the load through an equivalent nonlinear element. Fig. 11 shows the proposed model for the FHA-C mini servo actuator setup.

The equivalent system consists of a drive side,  $m_1$ , composed of the motor and wave-generator inertia, an equivalent dynamic spring,  $k_{eq}$ , and an inertia load,  $m_3$ . The identification of the equivalent spring is carried out by locking the output side of the actuator and prescribing a random input excitation to the system similar to the torsional stiffness measurement procedures in a harmonic drive. The applied torque and the angular displacement of the input side of the gear system are then measured, whereas the drive side inertia can be obtained from the catalogue values provided by the manufacturer.

Fig. 12 shows the plot of the torque against the displacement from the locked-load experiment excited by a random input with 1 Hz frequency bandwidth. From the figure, we can conclude that the torsional stiffness with a pre-sliding friction hysteresis is still playing an important role. Based on this assumption, the hysteresis is modeled in order to be able to calculate the equivalent dynamic parameters (1) and (2).

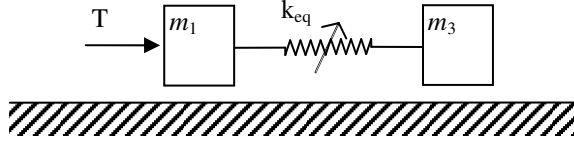


Fig. 11. Second approach model of the setup. The load is represented by  $m_3$  and the equivalent dynamic parameter is denoted by  $k_{eq}$ . The output shaft connecting the flexspline to the load is assumed to be rigid.

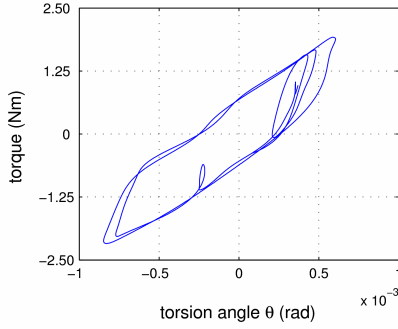


Fig. 12. Equivalent nonlinear stiffness behavior of the simplified FHA-C mini servo actuator model.

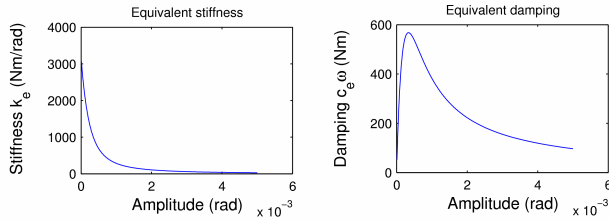


Fig. 13. The dynamic equivalent parameters of the hysteresis parts in the torsional stiffness of the FHA-C mini servo actuator.

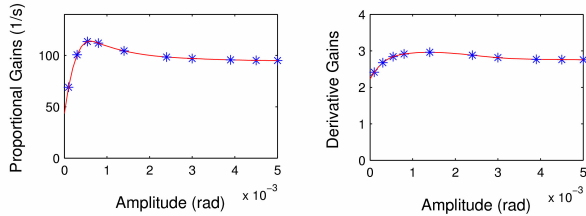


Fig. 14. Scheduled PD gains for the second approach model developed based on the equivalent dynamic parameters.

For gain scheduling control purposes, however, it should be mentioned here that the adjustment of the gains remains scheduled discretely every time the relative motion between two blocks  $m_1$  and  $m_3$  is reversed, since the equivalent dynamic parameters of the system are developed based on the amplitude of the relative displacement between the drive side,  $m_1$ , and the load side,  $m_3$ .

Based on the equivalent dynamic parameters in Fig. 13, PD gains at different selected relative amplitudes between two encoder readings are optimized considering the designated performance criteria. Afterwards, the gains are interpolated for other intermediate amplitudes as shown in Fig. 14.

Fig. 15 shows the step response to a 0.4 rotation step input ( $0.4 \times 2\pi$  rad  $\approx 2.513$  rad) of the system with the second approach of the gain scheduling controller. The response is plotted in the greyed figure of the previous controllers' results in order to have straight comparison between the performances of all the controllers. The steady state error falls higher than that of the previous experiments. This can be understood since this approach neglects the friction force that may occur in the system, including the friction in the output shaft, which is obviously not considered in the equivalent hysteresis spring of the model.

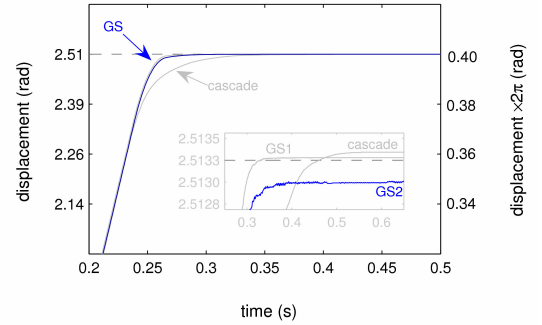


Fig. 15. Step response to a 2.513 rad step input of the system modeled by the second approach with the gain scheduling (GS).

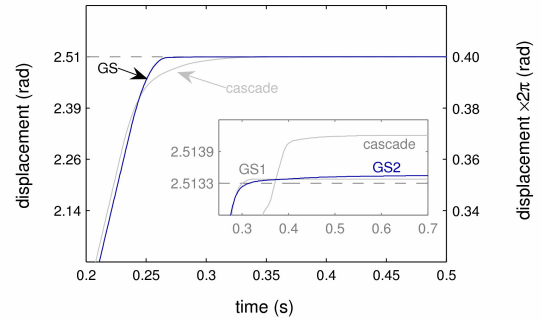


Fig. 16. Step response to a 2.513 rad step input of the system with additional load using the gain scheduling (GS) of the second approach.

TABLE II.  
PERFORMANCE OF THE SECOND APPROACH GAIN SCHEDULING CONTROLLER.

Object	Step input (rad)	Rise time <sup>1</sup> (s)	Error (rad)
No Load	2.513	0.25	$2.404 \times 10^{-4}$
Loaded	2.513	0.26	$2.230 \times 10^{-4}$

<sup>1</sup> The time to take the system to 1% of the set point.

The step responses for the increased inertia object case to 2.513 is depicted in Fig. 16. In this experiment, the second approach controller yields comparable results to the first approach gain scheduling controller. Table II summarizes the performance quantification of the second approach gain scheduling controller for the different

operation conditions. Evaluating robustness of the controllers can be considered in two different perspectives. In the first consideration, a system is said to be robust if a maximum (steady state) error for various operating conditions (for example, with or without load) lies within a certain tolerable limit, without considering how the error values deviate in different operating conditions. The second perspective considers the deviation of errors at various operating conditions as a measure of robustness of a system. A system is said to be robust if the deviation of errors of the system stay within certain limit for various operating conditions. Fig. 17 illustrates the two criteria in evaluating robustness.

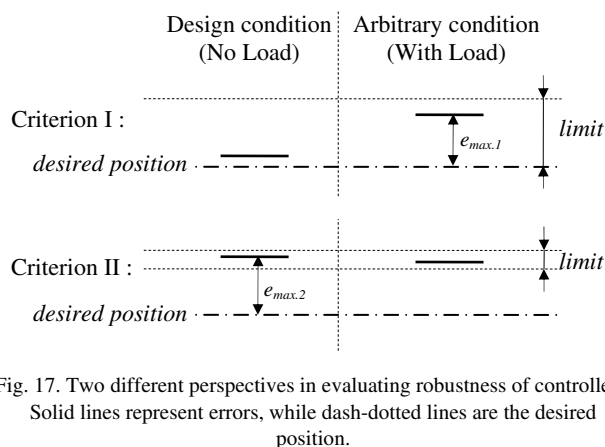


Fig. 17. Two different perspectives in evaluating robustness of controllers. Solid lines represent errors, while dash-dotted lines are the desired position.

## V. CONCLUSIONS

The FHA-C mini servo actuator system is presented in a complete package causing significant difficulty in identifying each component separately. Two simplified models are proposed to overcome this difficulty. The first model considers the system as a single mass subjected to frictional force. The friction is attributed to the moving components, such as the bearings, in the system.

In the second model, the system is considered as two-degree-of-freedom system, where the two lumped masses are connected by an equivalent spring element. Frictional losses in the motor side, gear mesh and torsional stiffness of the gearing system manifest themselves simultaneously in the equivalent spring element of the second simplified model.

As to the position control problem, two types of controllers have been studied, namely a cascade controller and gain scheduling controllers. The gain scheduling results in superior performance. Both approaches of the gain scheduling techniques offer good and comparable results. However, it has to be mentioned that the first approach is relatively simpler to identify and implement, while the second approach also requires two encoders to control the system.

## ACKNOWLEDGMENT

The authors acknowledge the support of the company Harmonic Drive AG, Germany, by providing the FHA-C mini servo actuator system and control during a long period of experimental investigation.

## REFERENCES

- [1] Harmonic Drive Technologies, (1994). *Harmonic Drive Gearing: Cup Type HDUC and HIUC Component Sets*, HD Systems, Inc., Hauppauge, New York.
- [2] Harmonic Drive Technologies, (1994). *Pancake Component Gear Sets*, HD Systems, Inc., Hauppauge, New York.
- [3] T. Tjahjowidodo, F. Al-Bender, and H. Van Brussel, "Modeling and Identification of Nonlinear Torsional Stiffness in Harmonic Drive", *The Proceedings of 5<sup>th</sup> Euromech Nonlinear Dynamics Conference*, Eindhoven, 2005, pp. 1809-1816.
- [4] T. Hidaka, T. Ishida, Y. Zhang, M. Sasahara, and Y. Tanioka, "Vibration of a Strain-Wave Gearing in an Industrial Robot", *Proc. of the International Power Transmission and Gearing Conference*, 1990, pp. 789-794.
- [5] D. P. Volkov, Y. N. and Zubkov, "Vibrations in a Drive With a Harmonic Gear Transmission", *Russian Engineering Journal*, 58(5), 1978, pp. 11-15.
- [6] H.D. Taghirad, *On the modeling and identification of harmonic drive system*, PhD thesis, Centre for Intelligent Machines, McGill University, Montréal, Québec, Canada, 1997.
- [7] W. Seyfferth, A.J. Maghzal and J. Angeles, "Nonlinear Modeling and Parameter Identification of Harmonic Drive Robotic Transmissions", *Proc. of IEEE International Conference on robotics and Automation*, 3, 1995, pp. 3027-3032.
- [8] H.D. Taghirad and P.R. Bélanger, "Robust Friction Compensation for Harmonic Drive Transmission", *Proceedings of 1998 IEEE International Conference on Control Applications*, 1998, pp. 547-551, Trieste, Italy.
- [9] H.D. Taghirad and P.R. Bélanger, "Kalman Filter Torque Sensing Technique for Harmonic Drives", *Proceedings of the 3rd International Conference on Industrial Automation 1*, Montreal, Canada, 1998, pp. 13.1-13.4.
- [10] R. Dhaouadi, "Torque Control in Harmonic Drives with Nonlinear Dynamic Friction Compensation", *Journal of Robotics and Mechatronics*, 16(4), 2004, pp. 388-396.
- [11] J.P. Hauschild, G. Hepler, and J. McPhee, "Friction Compensation of Harmonic Drive Actuators", *Proceedings of 6th International Conference on Dynamics and Control of Systems and Structures in Space*, Liguria, Italy, 2004, pp. 683-692.
- [12] T. Tjahjowidodo, *Characterization, Modelling and Control of Mechanical Systems Comprising Material and Geometrical Nonlinearities*, PhD thesis, Department Werktuigkunde Katholieke Universiteit Leuven, Belgium, 2006.
- [13] T. Tjahjowidodo, F. Al-Bender, W. Symens, and H. Van Brussel, "A Gain Scheduling Controller for Friction Compensation", to be submitted in *IEEE Trans. of Automation*, 2007.
- [14] F. Al-Bender, W. Symens, J. Swevers and H. Van Brussel, H, "Theoretical Analysis of the Dynamic Behavior of Hysteresis Elements in Mechanical Systems", *International Journal of Non-Linear Mechanics*, 39, 2004, pp. 1721-1735.
- [15] W.D. Iwan, "A Distributed-Element Model for Hysteresis and Its Steady-State Dynamic Response", *Journal of Appl. Mech.*, 33, 4, 1966, pp. 893-900.
- [16] R.H. Macmillan, *Non-Linear Control System Analysis*, Pergamon Press, Oxford, 1962.